

DOI: 10.1002/cphc.200((will be filled in by the editorial staff))

Effect of Magnesium Bond on the Competition between Hydrogen Bond and Halogen Bond and the Induction of Proton and Halogen Transfer

Hui-Li Xu,^[a] Qing-Zhong Li,^{*[a]} and Steve Scheiner^{*[b]}*((Dedication, optional))*

HOX (X = Cl, Br, I, and At) can engage in either a H-bond (HB) or halogen bond (XB) with a base like HCN, NH₃, and imidazole. While the former is energetically preferred for X=Cl and Br, it is the XB that is more stable for At, with I showing little preference. MgY₂ forms a Mg-bond with the O atom of HOX, which grows stronger in the order X= Cl < Br < I < At and Y= F < Cl < Br. When all three molecules are

combined together, both the Mg and the H/X bonds are cooperatively strengthened to a large degree. Rather than causing a reversal in the HB/XB competition, the Mg-bond acts primarily to amplify the natural preference within the dimer. The Mg-bond induces a certain degree of transfer from O to N of the bridging atom in the H/X bond. Comparison is also made with the effects of a Be-bond.

1. Introduction

Because many noncovalent forces are of comparable strength, there can sometimes be a healthy competition as to which might predominate in a given setting. As one example, the competition between intra- and intermolecular hydrogen bonds (HBs) play a crucial role in determining the molecular recognition properties of diarylureas^[1] as well as many other systems. The halogen bond (XB) is a related sort of noncovalent interaction that represents a major factor in constructing supramolecular materials^[2,3] and promoting chemical reactions.^[4,5] As the XB strength is comparable to that of the HB, numerous studies have evaluated the competition between these two types of bonds^[6-14]. This competition is not always a straightforward one. For one thing, their relative strengths can depend upon the nature of the base. When difluoriodomethane binds with trimethylamine (TMA) and dimethylether (DME), both H- and X-bonded complexes appear simultaneously, but the latter is more stable than the former for TMA while the reverse is true for DME, while at the same time, methyl fluoride prefers to form HBs.^[6] The situation gets further complicated when difluoriodomethane is replaced by

fluoriodomethane, in that only the H-bonded complex occurs for both DME and TMA.^[7] These observations indicate that the mere addition of a single F substituent can exert a strong influence upon the HB/XB competition. The nature of the solvent plays a role as well. Polar solvents have a reverse effect on the relative strengths of the HB and XB, and can change H-bonded co-crystals in the least polar solvents to X-bonded co-crystals in more polar solvents, depending on the relative strength of the two interactions.^[14]

Hypohalous acid (HOX, X = halogen) represents an ideal model by which to study the fundamental aspects of this competition.^[15-28] It is a small molecule, and can easily engage in either a HB or XB. In general, HOX forms a stronger HB when X = Cl and Br, while the XB becomes competitive for X = I. HOX offers further intriguing behavior in that HOBr preferly forms a HB with H₂CO,^[22] but a XB with H₂CS.^[23] Upon increasing the solvent polarity, the HB becomes weaker and the XB stronger.^[23] This competition thus warrants more detailed scrutiny. Especially important, and scarcely studied to this point are the specifics of the way in which this competitive HB/XB behavior of HOX might be affected by the presence of a third molecule, an essential ingredient in understanding the effects of solvation.

Indeed, cooperativity is an essential property of noncovalent interactions not only in terms of solvation but also in the fields of crystal materials, chemical reactions, and molecular recognition.^[29-31] For instance, assembly of molecules on surfaces can be steered by cooperative effects.^[32] It is thus not surprising that there has been some healthy study of cooperativity involving both HBs and XBs.^[33-43] which suggested that under certain conditions, the presence of both of these interactions within a single system can reinforce one another. For example, aromatic triazole foldamers stabilized by intramolecular CH...O H-bonding can efficiently bind neutral tri- and bidentate organohalogens through multiple N...X (X=Cl, Br, and I) XBs.^[44]

In studying the reaction of LiNH₂ with MgH₂, the concept of a magnesium bond (MgB) was proposed,^[45] which comprises the

[a] Dr. H. Xu, Q. Li
Laboratory of Theoretical and Computational Chemistry and School of Chemistry and Chemical Engineering, Yantai University
Yantai 264005(China)
Fax: (+86)535-6902063
E-mail: lj70316@sohu.com

[b] Prof. S. Scheiner
Department of Chemistry and Biochemistry, Utah State University,
Logan, UT 84322-0300 (USA)
E-mail: steve.scheiner@usu.com

Supporting information for this article is available on the WWW under <http://www.chemphyschem.org> or from the author. **((Please delete if not appropriate))**

interaction between an acidic Mg atom on one molecule and a negative site in another molecule, analogous to a HB or XB. Later work expanded this concept to the idea of a π -MgB between MgX_2 ($X = \text{H}, \text{F}$) and acetylene, ethylene, and benzene^[46] where the π -system of the latter molecules act as an electron donor. The calculations^[46] pointed to electrostatics and polarization as the primary stabilizing forces. A more recent study^[47] of MgBs considered the interactions between MgCl_2 and FH , ClH , BrH , H_2O , H_2S , NH_3 , and PH_3 , which found the strongest bond with NH_3 and H_2O , with interaction energies exceeding 25 kcal/mol. MgH_2 forms a cyclic complex with LiNH_2 ,^[45] which includes both a $\text{Mg}\cdots\text{N}$ MgB and a $\text{Li}\cdots\text{H}$ HB, with some elements of cooperativity between the two.

This work focuses on the HOX series, with halogen atom X varying from Cl all the way down the periodic table to At. The HOX molecule can engage in either a HB or XB, and is small enough to avoid complications from secondary interactions. The consideration of four different X atoms permits a careful examination as to how the property of this atom affects both the HB and XB, and the competition between the two bonds. Three different bases, of varying size and strength, are paired with HOX in order to determine if the base affects the relative stabilities of the two bonds. So as to introduce elements of cooperativity into the study, the MgY_2 molecule is added which engages in a MgB with the HOX O atom. Three different halogen Y atoms are considered to again elucidate how the strength of this MgB interacts with the HB/XB competition. By employing a full range of theoretical techniques, including energy decomposition, analysis of molecular electrostatic potential and electron density topology, and NBO interorbital charge transfer, one is able to arrive at a full picture of the origins of the energetics and geometries that emerge from the calculations.

2. Theoretical Methods

The geometries of complexes and monomers were optimized at the second-order Møller–Plesset perturbation theory (MP2) level with the aug-cc-pVTZ basis set for all atoms, except the iodine and astatine, for which the aug-cc-pVTZ-PP basis set was used^[48-50] which include relativistic effects. Harmonic frequency calculations were then performed at the same level to confirm that the obtained structures correspond to true energy minima on the potential energy surfaces. The interaction energy was calculated as the difference between the energy of the complex and the energy sum of the respective monomers with their geometries frozen as in the complex. The interaction energy was corrected for basis set superposition error (BSSE) by the counterpoise method of Boys and Bernardi.^[51] All calculations were carried out with the Gaussian 09 suite of programs.^[52]

Molecular electrostatic potentials (MEPs) on the 0.001 electrons Bohr⁻³ contour of electronic density were obtained at the MP2/aug-cc-pVTZ level with the wave function analysis-surface analysis suite (WFA-SAS) program.^[53] The Natural Bond Orbital (NBO) treatment^[54] was used to analyze charge-transfer interactions between occupied and virtual orbitals at the HF/aug-cc-pVTZ level. Topological properties of complexes were analyzed by employing the Atoms in Molecules (AIM) methodology^[55] with the AIM2000 program.^[56] Energy decomposition analysis (EDA) was carried out at the MP2/aug-cc-pVTZ level to obtain insight into the nature of the interactions using the GAMESS program^[57] with the localized molecular orbital-energy decomposition analysis (LMOEDA) method.^[58] Non-covalent interaction (NCI) analysis was performed using the

Multifwfn program^[59] and the related plots were graphed using the VMD program.^[60]

Table 1. The most positive MEPs (V_{max}) on the H and X atoms of HOX and on the Mg atom of MgY_2 as well as the negative MEP (V_{min}) on the N atom of the nitrogenated base and on the O atom of HOX, all are in kcal·mol⁻¹.

	$V_{\text{max-H}}$	$V_{\text{max-X}}$	$V_{\text{min-O}}$		$V_{\text{min-N}}$	$V_{\text{max-Mg}}$
HOCl	62.05	25.98	-21.19	HCN	-33.60	MgF_2 180.95
HOBr	59.49	35.51	-23.19	NH_3	-39.58	MgCl_2 124.64
HOI	55.27	47.32	-26.78	IM	-45.43	MgBr_2 105.22
HOAt	50.64	58.46	-30.58			

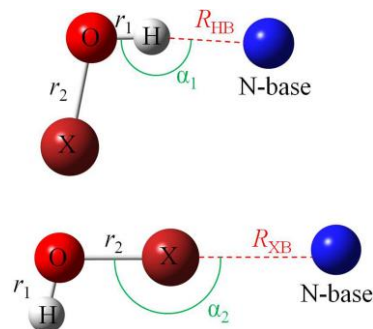


Figure 1. Structures of H-bonded (up) and X-bonded (down) complexes.

3. Results and Discussion

3.1. Dependence of HB and XB on the X Atom and Lewis Bases

Table 1 presents the most positive MEPs (V_{max}) around the H and X atoms of HOX and the most negative MEP (V_{min}) on the N atom of three Lewis bases HCN, NH_3 , and imidazole (IM). Due to its lesser electronegativity and higher polarizability, the heavier X atom leads to a smaller $V_{\text{max-H}}$ value on the H atom but a larger $V_{\text{max-X}}$ on the X atom. The MEP associated with the H atom is more positive than that for the X atom for $X = \text{Cl}, \text{Br}, \text{and I}$ but the reverse is true for $X = \text{At}$. Table 1 shows that $V_{\text{max-X}}$ is considerably more sensitive to the nature of X than is $V_{\text{max-H}}$. As one progresses from HCN to NH_3 to IM, there is a clear pattern of intensification of $V_{\text{min-N}}$ on the N atom, suggesting a growing base strength.

It has been demonstrated that both H and X atoms in HOX can respectively participate in a HB and a XB with nitrogen bases.^[20] Moreover, the former is stronger than the latter, with the exception of $X = \text{At}$.^[20] As a starting point for the work to be described below, some of those calculations were repeated here, but adding the much stronger imidazole base, with the considerably more negative $V_{\text{min-N}}$ (see Table 1). **Their schemes are displayed in Figure 1.**

Table 2. Interaction energies (ΔE) of HB and XB as well as their difference ($\Delta E_{\text{XB}} - \Delta E_{\text{HB}}$) in the binary systems, in kcal·mol⁻¹

dyads	ΔE_{HB}	ΔE_{XB}	$\Delta E_{\text{XB}} - \Delta E_{\text{HB}}$
HOCl...HCN	-6.67(1)	-2.57(13)	4.10
HOCl... NH_3	-11.30(2)	-4.47(14)	6.83
HOCl...IM	-12.95(3)	-5.87(15)	7.08
HOBr...HCN	-6.53(4)	-3.98(16)	2.55
HOBr... NH_3	-11.05(5)	-7.47(17)	3.58
HOBr...IM	-12.72(6)	-9.91(18)	2.81
HOI...HCN	-6.29(7)	-5.78(19)	0.51
HOI... NH_3	-10.60(8)	-10.45(20)	0.15
HOI...IM	-12.32(9)	-13.82(21)	-1.50
HOAt...HCN	-5.84(10)	-7.78(22)	-1.94
HOAt... NH_3	-9.84(11)	-12.82(23)	-2.98
HOAt...IM	-11.43(12)	-16.76(24)	-5.33

Since a number of these dimers have been reported earlier,^[20] geometric details will not be repeated here. Table 2 presents the interaction energies of both the HB and XB configurations which strengthen in the same $\text{HCN} < \text{NH}_3 < \text{IM}$ order as the values of

$V_{\min-N}$ in Table 1. With regard to relative strength, the HB complexes are more strongly bound than their XB counterparts for the smaller X atoms. This difference is underscored by the last column of Table 2 which displays the energetic preference for the HB vs the XB. This preference lies in the 4-7 kcal/mol range for X=Cl, and is reduced to less than 4 kcal/mol for X=Br. Any such preference essentially disappears when X=I, and reverses to a preference for the XB for the largest halogen At. This pattern is quite consistent with the MEP values in Table 1 where $V_{\max-H}$ exceeds $V_{\max-X}$ for the three smaller halogen atoms, but the reverse is true for At. On a more subtle level, the difference between HB and XB interaction energies shows an interesting sensitivity to the nature of the base. For X=Cl, the strongest base leads to the greatest preference for the HB. This trend vanishes for X=Br and then reverses for X=I and At, where the stronger base yields the largest preference for the XB. These trends can be understood on the basis of the idea that the stronger base, with its more negative $V_{\min-N}$, will in turn be more sensitive to any distinctions between $V_{\max-H}$ and $V_{\max-X}$. This behavior of the two interaction energies is exhibited graphically in Figure 2 which emphasizes the greater sensitivity of the XB vs the HB to the identity of the X atom.

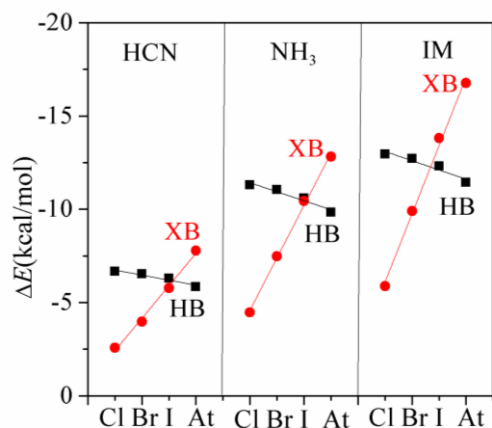


Figure 2. Dependence of interaction energies of H-bond and X-bond on the halogen atom in the binary systems.

Decomposition of each interaction energy into its composite parts in Table S1 shows first that the electrostatic component is universally the largest, followed by polarization and lastly by dispersion, whether HB or XB. It is of greatest interest to see how these two bonds compare with one another with respect to each of these components separately. The last three columns of Table S1 report the change in each quantity upon rearrangement of the dimer from HB to XB. The first three rows for example, show that both the electrostatic and polarization terms become less negative for the XB whereas there is an increase in the dispersion energy. Indeed the greater dispersion energy of the XB is true for all complexes, but not so for the other two quantities. As the X atom grows in size, there is a progressively greater enhancement of both ΔE^{ele} and ΔE^{pol} for the XB, relative to the HB. The same can be said for raising the basicity from HCN to NH_3 to IM. This pattern reaches its zenith for the HOAt...IM dimer where the electrostatic and polarization energies of the XB exceed that of the HB by 20 and 13 kcal/mol, respectively. These effects can be traced to the rising polarizability and diminishing electronegativity as the halogen atom is enlarged.

The presence of the HB/XB is further evidenced by a colored disk between the H/X atom of HOX and the N atom of the base in the NCI analyses (Figure S1). The color of this disk becomes deeper blue in the order $\text{HCN} < \text{NH}_3 < \text{imidazole}$, indicative of a

stronger interaction. In the HB complexes of $\text{HOX}\cdots\text{imidazole}$, a secondary $\text{H}\cdots\text{X}$ interaction is also found, as seen by a green region between the two atoms. This green region is larger for the heavier X atoms, indicating that the $\text{H}\cdots\text{X}$ interaction is stronger. However, the energy of the strongest $\text{H}\cdots\text{X}$ interaction is calculated to be only $-0.24 \text{ kcal mol}^{-1}$ in $\text{HOAt}\cdots\text{imidazole}$ based on the method proposed by Espinosa and coauthors.^[61] Thus the contribution of these secondary $\text{H}\cdots\text{X}$ interactions can be safely ignored in the HB complexes of $\text{HOX}\cdots\text{imidazole}$.

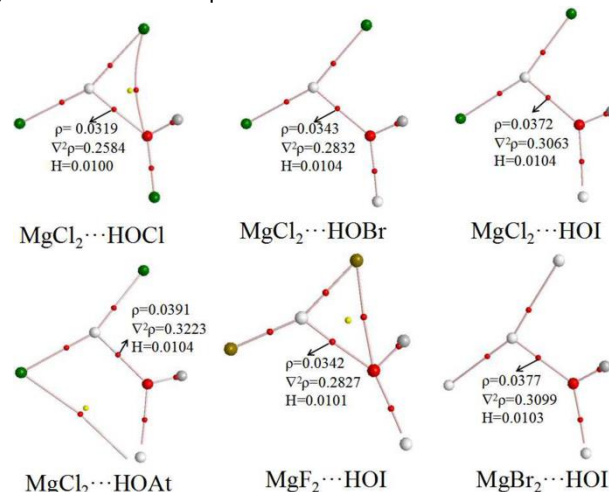


Figure 3. AIM diagrams of $\text{MgY}_2\cdots\text{HOX}$, the topological parameters are given in au.

3.2. Dependence of Mg-bond on the Halogen Atom

Previous study of the magnesium bond (MgB) utilized MgCl_2 and MgBr_2 in both $\text{Lp-MgB}^{[47]}$ and $\pi\text{-MgB}^{[46]}$ forms. This work focuses on the former by combining MgY_2 ($Y = \text{F}, \text{Cl}, \text{and Br}$) with the HOX molecules mentioned above. AIM diagrams of these dimers are presented in Figure 3 which shows a $\text{Mg}\cdots\text{O}$ bond path in all six complexes. There are secondary bond paths in several, for example an $\text{At}\cdots\text{Cl}$ bond in $\text{MgCl}_2\cdots\text{HOAt}$, but these bonds are assessed as quite weak based upon the electron density at their bond critical points (BCPs). So attention is drawn to the $\text{Mg}\cdots\text{O}$ bonds whose BCP characteristics are presented in Figure 3. The positive Laplacian and energy density are comparable to those of other $\text{Lp-MgBs}^{[47]}$ which may be characterized as a closed-shell interaction.^[62] As one varies the X atom of $\text{MgCl}_2\cdots\text{HOX}$ from Cl up to At, there is a steady increase in both ρ_{BCP} and $\nabla^2\rho$, signs of growing bond strength. One also sees the bond gaining strength when the Y atom of $\text{MgY}_2\cdots\text{HOI}$ enlarges from F to Cl to Br. In other words, increasing the electronegativity of the substituent on HOX weakens the MgB, whereas the opposite is true for the substituents attached to Mg. This pattern is sensible in light of the fact that HOX and MgY_2 serve as electron donor and acceptor, respectively. **Of course, AIM bond paths are not infallible indicators of bonds, as some have pointed out.^[63-66] However, they do offer a generally useful and extensively applied measure of bond strength.**

dyads	$R(\text{Mg-O})$	ΔE	$\text{CT}^{[a]}$	$E^2^{[b]}$	θ
$\text{MgCl}_2\cdots\text{HOCl}$	2.101	-19.05	0.0117	14.04	159.28
$\text{MgCl}_2\cdots\text{HOBr}$	2.070	-20.59	0.0119	14.55	159.13
$\text{MgCl}_2\cdots\text{HOI}$	2.050	-23.07	0.0151	15.15	158.51
$\text{MgCl}_2\cdots\text{HOAt}$	2.035	-25.30	0.0167	15.93	156.77
$\text{MgF}_2\cdots\text{HOI}$	2.068	-21.59	0.0070	10.27	157.68
$\text{MgBr}_2\cdots\text{HOI}$	2.046	-23.23	0.0124	16.29	158.72
$\text{MgCl}_2\cdots\text{HOI}$	2.050	-23.07	0.0151	15.15	158.51

[a] CT is the sum of the charges on all atoms of HOX in the dyads.

[b] E^2 corresponds to the two $\text{Lp}_O \rightarrow \sigma^*_{\text{Mg-Y}}$ orbital interaction in the dyads

except $\text{MgF}_2 \cdots \text{HOI}$, where it is $\text{Lp}_N \rightarrow \text{Lp}^*_{\text{Mg}}$.

These same trends appear in other facets of these complexes. As reported in Table 3, the $R(\text{Mg} \cdots \text{O})$ distance grows shorter and the interaction energy becomes more negative for the heavier X atom, and the smaller Y atom (although there is a small reversal between $\text{Y}=\text{Cl}$ and Br). The two measures of charge transfer echo these trends. Both the total transfer from one molecule to the other, CT, and the NBO diagnosis of interorbital transfer from the O lone pair to the pair of $\sigma^*(\text{Mg}-\text{Y})$ orbitals in the last column of Table 3 strengthen as indicated by the other measures. (Again, there is the discrepancy between $\text{Y}=\text{Cl}$ and Br , noted above for R and ΔE .) Finally, these trends can also be traced to the growing value of $V_{\text{min-O}}$ near the O atom in Table 1 as the X substituent in HOX becomes less electronegative. The irregularity observed between $\text{Y}=\text{Cl}$ and Br may be due in part to the nonlinearity introduced into the MgY_2 molecule by its interaction with HOX, as may be seen by the $\theta(\text{Y}-\text{Mg}-\text{Y})$ angles reported in the last column of Table 3.

The origin of the $\pi\text{-MgB}^{[46]}$ was previously examined by an energy decomposition method, and the results showed that electrostatic energy is the largest contributor. For purposes of comparison, the interaction energies of the $\text{Lp}-\text{MgB}$ in the $\text{MgY}_2 \cdots \text{HOX}$ dyads were similarly decomposed into five physical terms: electrostatic, exchange, repulsion, polarization, and dispersion energies (Table S2). As in the $\pi\text{-MgB}$, electrostatic energy is again the largest term in the $\text{Lp}-\text{MgB}$, corresponding to 65-74% of the sum of electrostatic, polarization, and dispersion energies. Polarization energy is slightly less than half of the magnitude of the electrostatic energy, while dispersion energy is negligible.

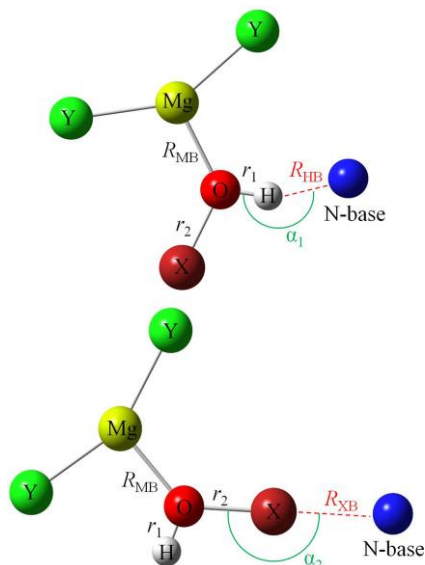


Figure 4. Structures of the ternary systems with a Mg-bond and a H-bond (up)/X-bond (down).

3.3. Effect of MgB on the HB and XB

Given the similar energetics of the HB and XB described above, it would be interesting to examine how this competition might be modulated by the addition of a third molecule. Specifically, a series of MgY_2 molecules were added in such a position that it can engage in a MgB with the HOX O atom, as pictured in Figure 4. One can see from Table S3 that all the interactions, HB, XB, and MgB alike, are strengthened in the ternary systems. The MgB interaction energy rises by as much as 160%, while the HB and XB are enhanced by even more, up to four and five-fold, respectively. These enhancements are generally larger for both

the stronger N-base, and the lighter X atom on HOX. Perhaps a more quantitative measure of this effect is associated with the cooperativity energy, E_{coop} , displayed in Table S3. The negative quantities are rather large in magnitude, rising up to nearly -50 kcal/mol in one case.

Table 4. Interaction energies (ΔE) of H-bond (HB) and X-bond (XB) as well as their difference ($\Delta E_{\text{XB}} - \Delta E_{\text{HB}}$) in the ternary systems, all are in kcal·mol⁻¹.

triads	ΔE_{HB}	ΔE_{XB}	$\Delta E_{\text{XB}} - \Delta E_{\text{HB}}$
$\text{MgCl}_2 \cdots \text{HOCl} \cdots \text{HCN}$	-9.89(25)	-5.13(39)	4.76
$\text{MgCl}_2 \cdots \text{HOCl} \cdots \text{NH}_3$	-54.77(26)	-16.81(40)	37.96
$\text{MgCl}_2 \cdots \text{HOCl} \cdots \text{IM}$	-52.94(27)	-34.15(41)	18.60
$\text{MgCl}_2 \cdots \text{HOBr} \cdots \text{HCN}$	-9.38(28)	-7.01(42)	2.37
$\text{MgCl}_2 \cdots \text{HOBr} \cdots \text{NH}_3$	-25.78(29)	-20.87(43)	4.91
$\text{MgCl}_2 \cdots \text{HOBr} \cdots \text{IM}$	-34.00(30)	-28.79(44)	5.21
$\text{MgCl}_2 \cdots \text{HOI} \cdots \text{HCN}$	-8.61(31)	-11.86(45)	-3.25
$\text{MgCl}_2 \cdots \text{HOI} \cdots \text{NH}_3$	-21.16(32)	-22.74(46)	-1.58
$\text{MgCl}_2 \cdots \text{HOI} \cdots \text{IM}$	-25.87(33)	-32.13(47)	-6.25
$\text{MgCl}_2 \cdots \text{HOAt} \cdots \text{HCN}$	-7.92(34)	-15.40(48)	-7.48
$\text{MgCl}_2 \cdots \text{HOAt} \cdots \text{NH}_3$	-18.07(35)	-25.31(49)	-7.24
$\text{MgCl}_2 \cdots \text{HOAt} \cdots \text{IM}$	-21.88(36)	-34.31(50)	-12.42
$\text{MgF}_2 \cdots \text{HOI} \cdots \text{NH}_3$	-22.74(37)	-21.43(51)	1.31
$\text{MgBr}_2 \cdots \text{HOI} \cdots \text{NH}_3$	-21.82(38)	-22.92(52)	-1.10

The energetics of each bond within the context of the various trimers are reported in Table 4. With the benefit of the aforementioned cooperativity, the HB energy lies in the range of 8.6 - 54.8 kcal/mol, which compares to the XB range of 5.1 - 34.2 kcal/mol. The last column of Table 4 relates to the competition between these two bonds, i.e. the energetic advantage of one over the other. As in Table 2, positive values correspond to a preference for the HB structure. In summary, the HB is preferred for the first 6 rows of Table 4 wherein HOCl and HOBr combine with any of the 3 bases. The larger values in Table 4 indicate that the MgB amplifies this preference. While this amplification is rather minor for HCN, it is a great deal larger for NH_3 and IM. Taking $\text{HOCl} \cdots \text{NH}_3$ as an example, the preference of 6.83 kcal/mol rises to 38.0 kcal/mol when the MgB is added. Precisely the opposite effect arises for HOI and HOAt. In these cases, the entries in the last column of Table 4 are more negative than those in Table 2. In other words, the MgB leads to an enhanced preference for the XB over the HB. One can generalize these observations to the overall conclusion that the MgB simply enhances any preference that occurs for the simple dimer itself, and does so to a large magnitude.

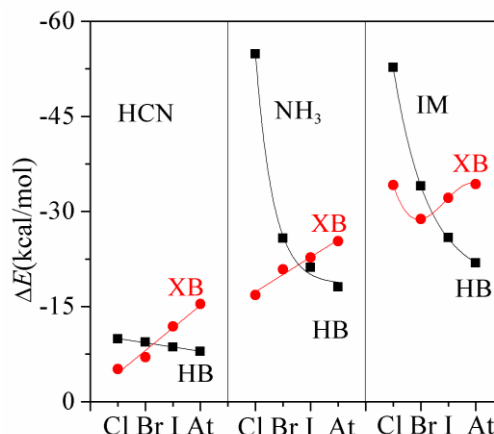


Figure 5. Dependence of interaction energies of H-bond and X-bond on the halogen atom in the ternary systems.

Comparison of Figure 5, which specifically includes the effect of the MgB, with Figure 2 offers a pictorial perspective of these patterns. In the case of the weak base HCN, the HB and XB curves are not substantially affected by the MgB. But one sees real differences for the two stronger bases. Rather than a fairly gradual decline in the HB energy as the X atom enlarges, this drop is precipitous when the MgB is present. The HB in $\text{HOX} \cdots \text{NH}_3$, for example, is reduced by 3 kcal/mol for $\text{X}=\text{Cl}$ to

X=At. But this same alteration in system reduces the HB energy by 33 kcal/mol after inclusion of the MgB. With respect to the XB, the influence of the MgB is much smaller. The same change from Cl to At in the above system has very little effect upon the XB energy.

Table 5. The most positive MEPs (V_{\max}) on the H and X atoms in $\text{MgY}_2 \cdots \text{HOX}$ and their changes (ΔV_{\max}) relative to the HOX monomer ($\text{kcal}\cdot\text{mol}^{-1}$).

dyads	$V_{\max\text{-H}}$	$V_{\max\text{-X}}$	$\Delta V_{\max\text{-H}}$	$\Delta V_{\max\text{-X}}$
$\text{MgCl}_2 \cdots \text{HOCl}$	78.38	51.41	16.32	25.43
$\text{MgCl}_2 \cdots \text{HOBr}$	77.79	62.71	18.29	27.20
$\text{MgCl}_2 \cdots \text{HOI}$	75.96	75.58	20.69	28.26
$\text{MgCl}_2 \cdots \text{HOAt}$	73.62	89.72	22.99	31.26
$\text{MgF}_2 \cdots \text{HOI}$	62.98	72.95	7.71	25.64
$\text{MgBr}_2 \cdots \text{HOI}$	73.82	75.67	18.54	28.35

One can seek insight into the reasons for these trends by consideration of how the σ -holes on the HOX molecule are affected by its formation of a MgB. The values of V_{\max} on the H and X atoms of HOX are displayed in the first two columns of Table 5 for the complexes of each molecule with MgY_2 . In all cases, the MgB enhances both of these σ -holes, by amounts listed in the last two columns of the Table. These increases are quite substantial, between 12 and 31% for the H σ -hole and even larger, in the 35%-50% range, for X. So as a first point, one would expect the formation of the MgB to strengthen both HB and XB. On a more refined level, $V_{\max\text{-H}}$ remains larger than $V_{\max\text{-X}}$ for HOCl and HOBr, but they are equal for HOI, and the latter exceeds the former for the remaining complexes in Table 5. In essence, the MgB tends to shift the balance away from the HB and toward the XB, at least on the basis of electrostatics. This behavior of the values of the MEP maxima is illustrated graphically in Figure S2.

The enhancement of both the HB and XB in the ternary systems can be further confirmed by the increase of the electron density at the corresponding bond critical point (Table S4). In more detail, Table S5 reports that the Laplacian is positive and energy density is negative for the dyad HBs, indicative of a partially covalent interaction.^[62] However, both the Laplacian and energy density are negative for the HB in most ternary systems (Table S6), suggesting that these HBs are covalent in nature.^[62] The XB in the binary systems of HOX (X = Br, I, and At) and $\text{NH}_3/\text{imidazole}$ exhibit the same bond properties as the HB in the binary systems. The XB in other binary systems is traditionally a closed-shell interaction, characterized by the positive Laplacian and energy density (Table S5). However, these XBs become a partially covalent interaction in the ternary systems with the exception in **39** (Table S6). Hence, the coexistence with a Mg-bond can affect the nature of HB and XB.

The MgB also causes prominent changes in the geometrical parameters of both the HB and XB. Comparison of the binding distances in the ternary systems (Table S7) and in the binary systems (Table S8) shows that all are shortened in the ternary systems, and by substantial amounts, up to ~ 0.6 Å. In almost all the binary systems, the XB is more linear than the HB, evidenced by the larger bond angle in the former (Table S8). The HB angle becomes smaller in the ternary systems except those involving imidazole, while the XB angle undergoes only a slight change in most ternary systems with the exception of imidazole complexes. In the binary systems, the O-H bond is elongated and the O-X bond is contracted for the HB, while the reverse occurs in the XB. Addition of the MgB amplifies these effects. Table S4 presents the change of the charge transfer for the HB and XB in the ternary systems relative to the binary systems. Clearly, the charge transfer is increased in the ternary systems. Figure 6 shows the relationship between the change of the charges transfer and the change of the interaction energy in the ternary systems. A strong correlation is observed between these terms,

especially for the HB, indicating the important role of charge transfer in strengthening these interactions.

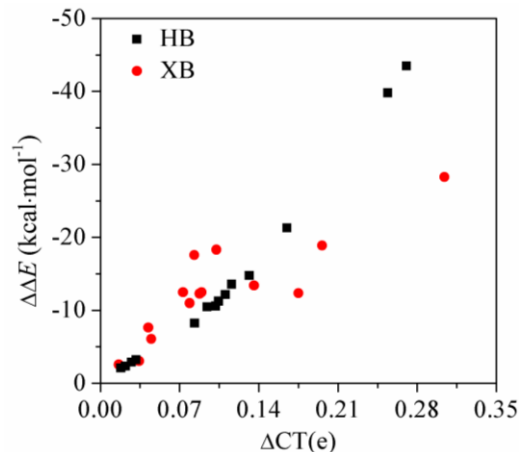


Figure 6. Change of charge transfer (ΔCT) versus change of interaction energy ($\Delta\Delta E$) for the H-bond and X-bond in the ternary systems.

3.4. Hydrogen/Halogen Transfer

Subsequent to formation of a HB, there is frequently the possibility that the bridging proton may transfer across to the base.^[67] Recent work suggests that a similar possibility exists in the case of halogen transfer within a XB.^[68] Due to the strengthening caused by a complementary MgB, it is worthwhile to examine such possibilities in the various triad systems. The optimized geometries of the some of these complexes are displayed in Figure 7. There is some evidence of proton transfer from HOCl to either NH_3 or IM when MgCl_2 engages in a MgB with the O atom. In both structures **26** and **27**, the bridging H lies closer to the N than to the O atom. When the HOCl molecule is reoriented so as to form a XB with IM in structure **41**, the Cl atom lies at the midpoint of the O \cdots N axis, so the Cl atom can be said to be roughly half-transferred. The same is true of **44** where the bridging Cl is replaced by Br.

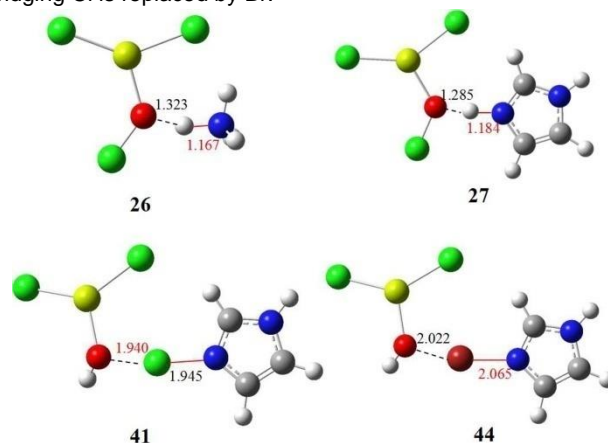


Figure 7. The optimized structures of **26**, **27**, **41**, and **44**. Distances are in Å.

These transfers and half-transfers have other symptoms and ramifications as well. In the binary HB/XB systems, the primary interorbital transfer involves the N lone pair and the $\sigma^*_{\text{O-H/O-X}}$ antibonding orbital. The alignment of these various orbitals is depicted on the left side of Figure 8. Upon proton transfer from O to N, the $\text{Lp}_\text{N} \rightarrow \sigma^*_{\text{O-H}}$ interaction transforms into its $\text{Lp}_\text{O} \rightarrow \sigma^*_{\text{N-H}}$ analogue, which may be seen in structures **26** and **27** (Figure 8). A similar transformation occurs in the partial halogen transfers in

41 and 42, although the lesser extent of the transfer results in a less drastic change in the character of the MOs.

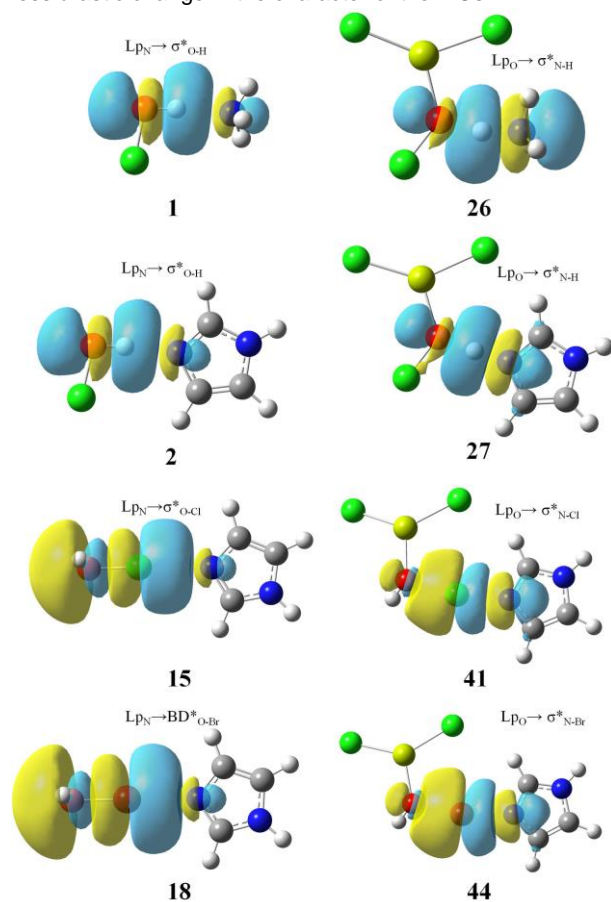


Figure 8. Schematic diagrams of orbital interactions.

4. Discussion and Conclusions

There are a number of aspects of these calculations whose accuracy can be evaluated by comparison with prior work. The Mg-bonded complexes of $\text{MgCl}_2 \cdots \text{LB}$ (LB = FH, ClH, BrH, H_2O , H_2S , NH_3 , PH_3) were compared using four different methods (B3LYP, M06-2X, MP2, CCSD(T)), and with two different basis sets (6-31+G(d), 6-311+G(3df,2p)).^[47] The MP2/6-31+G(d) intermolecular separations were closest to the CCSD/6-31+G(d) values.^[47] The smallest average deviation of the interaction energy with respect to CCSD(T) was obtained for the MP2 method.^[47] The authors suggested that the CCSD(T) method in conjunction with a larger 6-311+G(3df,2p) basis set might increase the interaction energy.^[47] Even so, their geometrics and energetics were discussed at the B3LYP/6-311+G(3df,2p) level in order to compare with the beryllium-bonded analogues.^[69] The interaction energy between MgX_2 (X = H, F) and acetylene, ethylene, or benzene was calculated at the MP2/aug-cc-pVTZ and CCSD(T)/aug-cc-pVTZ levels, and it was found that the MP2 results are in good agreement with those arising from the CCSD(T) method, and their differences do not exceed 7.1%.^[46] The interaction energies of HB and XB between HOI and NH_3 were respectively obtained as -10.78 and -10.86 kcal/mol at the MP2 level with a mixed basis set (def2-TZVPP for the I atom and 6-311++G(2d,2p) for the rest of the atoms),^[20] which are very close to our results obtained at the MP2/aug-cc-pVTZ(PP) level. More importantly, the MP2/aug-cc-pVTZ(PP) method has been used to successfully study many H-bonded and X-bonded

complexes involving HOX.^[19,22,23] Thus we believe our results based on the MP2/aug-cc-pVTZ(PP) method are reliable.

Certain characteristics of the MgB can be compared with its close cousin. A beryllium bond (BeB) was shown to be stronger than the corresponding MgB given the same base.^[47] Confirming some of our results above, previous studies have shown that transfer of a proton or halogen can also be promoted by a strong beryllium bond.^[70-73] When the hydroxyl O atom of acetic acid is engaged in a BeB with BeCl_2 , the hydroxyl H atom forms a stronger HB, which can also lead to proton transfer if the base is strong enough.^[70] When BeH_2 approaches the hydroxyl O atom of malonaldehyde, the intramolecular HB in the latter becomes stronger, leading to a proton transfer, whereas a reverse result is obtained if the carbonyl O atom binds with BeH_2 .^[71] The proton also moves across from the X atom of HX (X = F, Cl, Br, I) to the N atom of NH_3 when BeCl_2 binds with the X atom of HX.^[72] In terms of transfer of halogen atoms, the addition of a BeB strengthens the XB between ClF and a N-base (NCH_3 , NHCH_2), varying from a traditional XB to a chlorine-shared system, or even to an ion pair, depending on the strength of the BeB and the N-base.^[73]

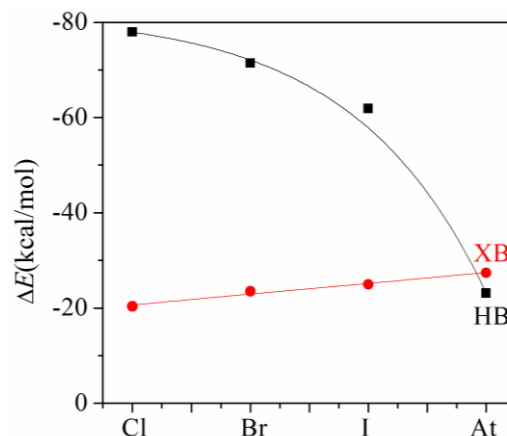


Figure 9. Dependence of interaction energies of H-bond and X-bond on the halogen atom in the system $\text{BeCl}_2 \cdots \text{HOX} \cdots \text{NH}_3$.

Given these general similarities it is particularly interesting to compare the influence of a BeB with a MgB on the competition between a HB and XB. The enhancing effect of a BeB on both the HB and XB within the $\text{BeCl}_2 \cdots \text{HOX} \cdots \text{NH}_3$ system was calculated and is illustrated in Figure 9, which may be compared directly with the Mg analogue in Figure 5b (central panel). Whether BeB or MgB, the addition of the third molecule enhances both the HB and XB. Where they differ, however, is in the sensitivity to the nature of the X atom. The enhancement of the XB energy upon going from X=Cl to At is similar for the MgB and BeB. However, the HB energy is reduced by some 60 kcal/mol by the BeB, nearly twice that in the Mg case. One sees from Table S9 that the BeB makes the XB more favorable than the HB when X = At, while this transition from HB to XB occurs for X=I for the MgB, even though the MgB is weaker than the BeB bond.

The BeB also produces a more pronounced proton transfer than does a MgB in $\text{BeCl}_2 \cdots \text{HOX} \cdots \text{NH}_3$ (X = Cl, Br, I), characterized by the comparative values of $r(\text{H} \cdots \text{N})$ and $r(\text{H} \cdots \text{O})$ (Figure S3). That is, the stronger second interaction facilitates this proton transfer. As in the Mg cases, there is no halogen transfer in $\text{BeCl}_2 \cdots \text{HOX} \cdots \text{NH}_3$ despite the stronger BeB. Replacement of MgCl_2 by the bare Mg^{2+} dication induces the halogen to transfer from the O to the N atom (Figure S3) owing to a very strong MgB. In the case of a HB, the likelihood of a proton transfer increases as the HB grows stronger. Such is not the case for halogen transfer. Although the heavier halogen atom engages in a

stronger XB than does its lighter analogues, it is the latter which is more prone to transfer.

In conclusion, the relative strength of the HB and XB in the HOX complexes depends on both the nature of the X atom and the basicity of the N-base. **Larger X atoms tend toward stronger halogen bonds due to their lesser electronegativity and greater polarizability. These same qualities make the H atom of HOX less positively charged, thereby reducing the HB strength. As a result, the HB complex is generally more stable, but this trend fades as X grows heavier, and actually reverses when X is the very large At atom.** The Mg \cdots O MgB from MgY₂ to HOX grows stronger as Y is enlarged and as X becomes smaller. These trends are consistent with basic concepts of electronegativity and polarizability. The function of HOX as simultaneous electron donor and acceptor in the MgY₂ \cdots HOX \cdots base triads leads to positive cooperativity and a surprisingly high level of strengthening of both bonds. The relative stabilities of the HB and XB noted in the dimers are amplified within the context of the triads. The addition of the MgB causes at least a partial migration of the bridging H/X within the respective HB/XB. In some cases, this motion is large enough so as to be characterized as a proton or halogen transfer.

Acknowledgements

This work was supported by the National Natural Science Foundation of China (21573188).

Keywords: Cooperativity; Molecular electrostatic potential, Energy decomposition, AIM, NBO

- [1] M. C. Etter, Z. Urbanczyk-Lipkowska, M. Zia-Ebrahimi, T. W. Panunto, *J. Am. Chem. Soc.* **1990**, *112*, 8415–8426.
- [2] J. W. Xu, X. M. Liu, J. K. P. Ng, T. T. Lin, C. B. He, *J. Mater. Chem.* **2006**, *16*, 3540–3545.
- [3] S. Y. Dong, B. Zheng, F. Wang, F. H. Huang, *Acc. Chem. Res.* **2014**, *47*, 1982–1994.
- [4] D. P. de Sousa, C. Wegeberg, M. S. Vad, S. Mørup, C. Frandsen, W. A. Donald, C. J. McKenzie, *Chem. Eur. J.* **2016**, *22*, 3810–3820.
- [5] J. W. Lee, M. T. Oliveira, H. B. Jang, S. Lee, D. Y. Chi, D. W. Kim, C. E. Song, *Chem. Soc. Rev.* **2016**, *45*, 4638–4650.
- [6] N. Nagels, Y. Geboes, B. Pinter, F. D. Proft, W. A. Herrebout, *Chem. Eur. J.* **2014**, *20*, 8433–8443.
- [7] Y. Geboes, F. D. Proft, W. A. Herrebout, *J. Phys. Chem. A* **2017**, *121*, 4180–4188.
- [8] W. K. Tian, Q. Z. Li, *Int. J. Quant. Chem.* **2015**, *115*, 99–105.
- [9] C. B. Aakeröy, M. Fasulo, N. Schultheiss, J. Desper, C. Moore, *J. Am. Chem. Soc.* **2007**, *129*, 13772–13773.
- [10] K. W. Rajewski, M. Andrzejewski, A. Katrusiak, *Cryst. Growth Des.* **2016**, *16*, 3869–3874.
- [11] J. Fanfrlík, J. Holub, Z. Růžičková, J. Řezáč, P. D. Lane, D. A. Wann, D. Hnyk, A. Růžička, P. Hobza, *ChemPhysChem* **2016**, *17*, 3373–3376.
- [12] S. W. L. Hogan, T. van Mourik, *J. Comput. Chem.* **2016**, *37*, 763–770.
- [13] S. Falcinelli, A. Bartocci, S. Cavalli, F. Pirani, F. Vecchiocattivi, *Chem. Eur. J.* **2016**, *22*, 764–771.
- [14] C. C. Robertson, J. S. Wright, E. J. Carrington, R. N. Perutz, C. A. Hunter, L. Brammer, *Chem. Sci.* **2017**, *8*, 5392–5398.
- [15] A. Zabardasti, Y. A. Tyula, H. Goudarziafshar, *J. Sulfur Chem.* **2017**, *38*, 119–133.
- [16] X. L. An, X. Yang, B. Xiao, J. B. Cheng, Q. Z. Li, *Mol. Phys.* **2017**, *115*, 1614–1623.
- [17] Q. Zhao, D. C. Feng, Y. M. Sun, J. C. Hao, Z. T. Cai, *J. Mol. Model.* **2011**, *17*, 1935–1939.
- [18] A. Zabardasti, A. Kakanejadifard, H. Goudarziafshar, M. Salehnassaj, Z. Zohrehband, F. Jaberansari, M. Solimannejad, *Comput. Theor. Chem.* **2013**, *1014*, 1–7.
- [19] G. Sánchez-Sanz, C. Trujillo, I. Alkorta, J. Elguero, *Phys. Chem. Chem. Phys.* **2012**, *14*, 9880–9889.
- [20] I. Alkorta, F. Blanco, M. Solimannejad, J. Elguero, *J. Phys. Chem. A* **2008**, *112*, 10856–10863.
- [21] F. Blanco, I. Alkorta, M. Solimannejad, J. Elguero, *J. Phys. Chem. A* **2009**, *113*, 3237–3244.
- [22] Q. Z. Li, X. S. Xu, T. Liu, B. Jing, W. Z. Li, J. B. Cheng, B. A. Gong, J. Z. Sun, *Phys. Chem. Chem. Phys.* **2010**, *12*, 6837–6843.
- [23] Q. Z. Li, B. Jing, R. Li, Z. B. Liu, W. Z. Li, F. Luan, J. B. Cheng, B. A. Gong, J. Z. Sun, *Phys. Chem. Chem. Phys.* **2011**, *13*, 2266–2271.
- [24] Q. Z. Li, J. L. Zhao, B. Jing, R. Li, W. Z. Li, J. B. Cheng, *J. Comput. Chem.* **2011**, *32*, 2432–2440.
- [25] Q. Z. Li, H. Li, J. H. Gong, W. Z. Li, J. B. Cheng, *Int. J. Quant. Chem.* **2012**, *112*, 2429–2434.
- [26] Q. Z. Li, R. Li, P. Guo, H. Li, W. Z. Li, J. B. Cheng, *Comput. Theor. Chem.* **2012**, *980*, 56–61.
- [27] Q. Z. Li, H. J. Zhu, H. Y. Zhuo, X. Yang, W. Z. Li, J. B. Cheng, *Spectrochim. Acta A* **2014**, *132*, 271–277.
- [28] Q. J. Tang, Z. F. Guo, Q. Z. Li, *Spectrochim. Acta A* **2014**, *121*, 157–163.
- [29] K. Kuwajima, *Proteins* **1989**, *6*, 87–103.
- [30] L. K. S. von Krbek, C. A. Schalley, P. Thordarson, *Chem. Soc. Rev.* **2017**, *46*, 2622–2637.
- [31] L. Tebben, C. Mück-Lichtenfeld, G. Fernández, S. Grimme, A. Studer, *Chem. Eur. J.* **2017**, *23*, 5864–5873.
- [32] H. Zhou, H. Dang, J. H. Yi, A. Nanci, A. Rochefort, J. D. Wuest, *J. Am. Chem. Soc.* **2007**, *129*, 13774–13775.
- [33] R. Montis, M. Arca, M. C. Aragoni, A. Bauzá, F. Demartin, A. Frontera, F. Isaia, V. Lippolis, *CrystEngComm* **2017**, *19*, 4401–4412.
- [34] M. Domagała, A. Lutyńska, M. Palusiak, *Int. J. Quant. Chem.* **2017**, *117*, e25348.
- [35] Q. Z. Li, Q. Q. Lin, W. Z. Li, J. B. Cheng, B. A. Gong, J. Z. Sun, *ChemPhysChem* **2008**, *9*, 2265–2269.
- [36] H. X. Liu, R. L. Man, Z. X. Wang, P. G. Yi, J. X. Zeng, *J. Theor. Comput. Chem.* **2013**, *12*, 1350028.
- [37] Q. Zhao, D. C. Feng, J. C. Hao, *J. Mol. Model.* **2011**, *17*, 2817–2823.
- [38] I. Alkorta, F. Blanco, P. M. Deyà, J. Elguero, C. Estarellas, A. Frontera, D. Quiñero, *Theor. Chem. Acc.* **2010**, *126*, 1–14.
- [39] T. Lankau, Y. C. Wu, J. W. Zou, C. H. Yu, *J. Theor. Comput. Chem.* **2008**, *07*, 13–35.
- [40] B. Jing, Q. Z. Li, R. Li, B. A. Gong, Z. B. Liu, W. Z. Li, J. B. Cheng, J. Z. Sun, *Comput. Theor. Chem.* **2011**, *963*, 417–421.
- [41] M. Solimannejad, M. Malekani, I. Alkorta, *Mol. Phys.* **2011**, *109*, 1641–1648.
- [42] S. J. Grabowski, *Theor. Chem. Acc.* **2013**, *132*, 1347.
- [43] P. P. Zhou, W. Y. Qiu, S. Liu, N. Z. Jin, *Phys. Chem. Chem. Phys.* **2011**, *13*, 7408–7418.
- [44] L. Y. You, S. G. Chen, X. Zhao, Y. Liu, W. X. Lan, Y. Zhang, H. J. Lu, C. Y. Cao, Z. T. Li, *Angew. Chem. Int. Ed.* **2012**, *51*, 1657–1661.
- [45] X. Yang, Q. Z. Li, J. B. Cheng, W. Z. Li, *J. Mol. Model.* **2013**, *19*, 247–253.
- [46] S. Y. Li, D. Wu, Y. Li, D. Yu, J. Y. Liu, Z. R. Li, *RSC Adv.* **2016**, *6*, 102754–102761.
- [47] R. Tama, O. Mó, M. Yáñez, M. M. Montero-Campillo, *Theor. Chem. Acc.* **2017**, *136*, 36.
- [48] P. I. Nagy, P. W. Erhardt, *J. Phys. Chem. A* **2006**, *110*, 13923–13932.
- [49] Z. X. Wang, C. Wu, H. X. Lei, Y. Duan, *J. Chem. Theory Comput.* **2007**, *3*, 1527–1537.
- [50] M. Huš, T. Z. Urbic, *J. Chem. Phys.* **2012**, *136*, 144305.
- [51] S. F. Boys, F. Bernardi, *Mol. Phys.* **1970**, *19*, 553–556.
- [52] M. J. Frisch, G. W. Trucks, H. B. Schlegel, G. E. Scuseria, M. A. Robb, J. R. Cheeseman, G. Scalmani, V. Barone, B. Mennucci, G. A. Petersson, H. Nakatsuji, M. Caricato, X. Li, H. P. Hratchian, A. F. Izmaylov, J. Bloino, G. Zheng, J. L. Sonnenberg, M. Hada, M. Ehara, K. Toyota, R. Fukuda, J. Hasegawa, M. Ishida, T. Nakajima, Y. Honda, O. Kitao, H. Nakai, T. Vreven, J. J. A. Montgomery, J. E. Peralta, F. Ogliaro, M. Bearpark, J. J. Heyd, E. Brothers, K. N. Kudin, V. N. Staroverov, R. Kobayashi, J. Normand, K. Raghavachari, A. Rendell, J. C. Burant, S. S. Iyengar, J. Tomasi, M. Cossi, N. Rega, J. M. Millam, M. Klene, J. E. Knox, J. B. Cross, V. Bakken, C. Adamo, J. Jaramillo, R. Gomperts, R. E. Stratmann, O. A. Yazyev, J. Austin, R. Cammi, C. Pomelli, J. W. Ochterski, R. L. Martin, K. Morokuma, V. G. Zakrzewski, G. A. Voth, P. Salvador, J. J. Dannenberg, S. A. Dapprich, D. Daniels, O. Farkas, J. B. Foresman, J. V. Ortiz, J. Cioslowski, D. J. Fox, Gaussian 09, Revision A.02, Gaussian, Inc. Wallingford, CT, **2009**.

- [53] F. A. Bulat, A. Toro-Labbe, T. Brinck, J. S. Murray, P. Politzer, *J. Mol. Model.* **2010**, *16*, 1679–1691.
- [54] A. E. Reed, L. A. Curtiss, F. Weinhold, *Chem. Rev.* **1988**, *88*, 899–926.
- [55] R. F. W. Bader, *Atoms in Molecules: A Quantum Theory*, Clarendon Press, Oxford, U.K. **1990**.
- [56] R. F. W. Bader, AIM2000 Program, v. 2.0, McMaster University, Hamilton, Canada, **2000**.
- [57] M. W. Schmidt, K. K. Baldridge, J. A. Boatz, S. T. Elbert, M. S. Gordon, J. H. Jensen, S. Koseki, N. Matsunaga, K. A. Nguyen, S. J. Su, T. L. Windus, M. Dupuis, J. A. Montgomery, *J. Comput. Chem.* **1993**, *14*, 1347–1363.
- [58] P. F. Su, H. Li, *J. Chem. Phys.* **2009**, *131*, 014102.
- [59] T. Lu, F. Chen, *J. Comput. Chem.* **2012**, *33*, 580–592.
- [60] W. Humphrey, A. Dalke, K. Schulten, *J. Mol. Graph.* **1996**, *14*, 33–38.
- [61] E. Espinosa, E. Molins, C. Lecomte, *Chem. Phys. Lett.* **1998**, *285*, 170–173.
- [62] W. D. Arnold, E. Oldfield, *J. Am. Chem. Soc.* **2000**, *122*, 12835–12841.
- [63] Z. A. Keyvani, S. Shahbazian, M. Zahedi, *Chem. Eur. J.* **2016**, *22*, 5003–5009.
- [64] M. Solimannejad, E. Bayati, M. D. Esrafil, *Mol. Phys.* **2014**, *112*, 2058–2062.
- [65] F. Weinhold, P. v. R. Schleyer, W. C. McKee, *J. Comput. Chem.* **2014**, *35*, 1499–1508.
- [66] I. Alkorta, G. Sanchez-Sanz, J. Elguero, *J. Phys. Chem. A* **2014**, *118*, 1527–1537.
- [67] B. Koeppel, S. A. Pylaeva, C. Allolio, D. Sebastiani, E. T. J. Nibbering, G. S. Denisov, H. H. Limbache, P. M. Tolstoy, *Phys. Chem. Chem. Phys.* **2017**, *19*, 1010–1028.
- [68] J. Crueiras, A. Ríos, *Phys. Chem. Chem. Phys.* **2016**, *18*, 30961–30971.
- [69] M. Yáñez, P. Sanz, O. Mó, I. Alkorta, J. Elguero, *J. Chem. Theory Comput.* **2009**, *5*, 2763–2771.
- [70] O. Mó, M. Yáñez, I. Alkorta, J. Elguero, *Mol. Phys.* **2014**, *112*, 592–600.
- [71] O. Mó, M. Yáñez, I. Alkorta, J. Elguero, *J. Chem. Theory Comput.* **2012**, *8*, 2293–2300.
- [72] M. Yáñez, O. Mó, I. Alkorta, J. Elguero, *Chem. Phys. Lett.* **2013**, *590*, 22–26.
- [73] I. Alkorta, J. Elguero, O. Mó, M. Yáñez, J. E. Del Bene, *Phys. Chem. Chem. Phys.* **2015**, *17*, 2259–2267.

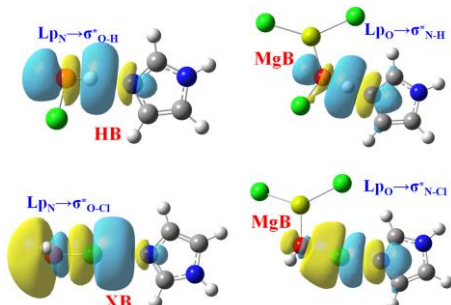
Received: ((will be filled in by the editorial staff))

Published online: ((will be filled in by the editorial staff))

Entry for the Table of Contents

ARTICLES

The function of HOX as simultaneous electron donor and acceptor in $\text{MgY}_2 \cdots \text{HOX} \cdots \text{base}$ results in positive cooperativity and a surprising strengthening of both bonds. The relative stabilities of the HB and XB in the dimers are amplified within the context of the triads. The addition of the MgB causes at least a partial migration of the bridging H/X within the respective HB/XB. In some cases, this motion is large enough so as to be characterized as a proton or halogen transfer.



Huili Xu, Qingzhong Li,* Steve Scheiner*

Page No. – Page No.

Effect of Magnesium Bond on the Competition between Hydrogen Bond and Halogen Bond and the Induction of Proton and Halogen Transfer